Investigations into Flow Rates of Opening Jet Plumes from a Fire Space

Takeyoshi TANAKA
DPRI, Kyoto University
Gokasho, Uji, Kyoto 611-0011, JAPAN

Jun-ichi YAMAGUCHI
Ohbayashi -Gumi Corporation
2-15-2 Konan, Minato-ku, Tokyo 108-8502, JAPAN

Takao WAKAMATSU
Science University of Tokyo
2461 Yamasaki, Noda-si, Chiba-ken, 278 Japan

ABSTRACT

A series of small scale and medium scale experiments were conducted to investigate the mass flow rates of buoyant jet plumes originating at wall openings from a fire space. From the results of the experiments, it was found that: (1)an opening jet plume can be modeled into a vertical plume as long as the mass flow rate is concerned provided that the entrainment height is adequately adjusted by the height of the plume virtual origin; (2)the height at which the mass flow rate of the vertical plume model becomes equal to the flow rate of the opening jet is 2/3 of the depth of the opening jet below the soffit, regardless the opening geometry; (3)the non-dimensional height of the virtual point source of an opening jet plume is only a function of the non-dimensional opening mass flow rate; and (4)the opening jet plume mass flow rates in experiments at two different scales are well correlated in terms of a non-dimensional plume mass flow rate and non-dimensional height, defined using the opening width as the characteristic length.

KEYWORDS: Opening jet plume, Entrainment, Scaling parameter, Non-dimensional flow rate

1. INTRODUCTION

Two layer zone fire models are now extensively used for scientific analyses of fire behavior and

for practical fire safety design of buildings[1]. However, some of the components of such fi models have not been sufficiently validated by experiments. The entrainment model of openin jet plumes is considered to be one of the component processes which needs further refinement.

In the event of fire, opening jets of hot gases form at various openings in a building and generat buoyant plumes once they enter into adjacent spaces, entraining surrounding air as they rise. Th entrainment of an opening jet plume has significant influence on the smoke behavior in th building but, despite the importance, a model for opening jet plume entrainment has not yet bee well established. The nature of an opening jet plume is more complex than that of a vertic buoyant plume: An opening jet plume is produced by an opening jet which has a horizont velocity and gets an upward velocity as soon as ejected from the opening; its entrainment may b affected by the wall above the opening and by the opening geometry. It is likely that theoretic and experimental investigations into the entrainment of opening jet plumes have been hindere by such complexities.

In this study, reduced scale experiments are conducted using two geometrically similar model fi compartments having different dimensions. The mass flow rates of opening jet plumes ar measured for various fire heat release rates and opening dimensions. A scaling parameter whic holds for calculation of the plume mass flow rates with any opening dimensions is also explored.

2. MEASUREMENT METHODOLOGY

Figure 1 illustrates the measurement system for the mass flow rate of opening jet plume employed in this study, which is similar to the experimental setup used by Zukoski et al. for th study of fire plumes[2]. This system consists of a burn room with an opening, a small hood and large hood. An opening jet plume is first captured by the small hood, which overflows to b captured again by the large hood. A mechanical extraction system is connected to the large hoo to exhaust the captured gases at such a rate that the gases from the small hood do not overflow th large hood. The primary role of the small hood is to get a sharp layer interface so that th entrainment height can be measured accurately.

Since the opening jet gases are diluted according to the amount of air entrained into the plume the plume flow rate can be obtained by measuring the gas concentrations in the opening jet, th small hood, the large hood, and measuring the flow rate in the exhaust duct. Considering th conservation of overall mass and species for the two hoods, the mass flow rates of the opening je $\dot{m}_D$ and the plume $\dot{m}_p$ can be expressed as a function of gas concentration Y and the mass flo rate in the duct $\dot{m}_E$ as follows:

$$\dot{m}_D / \dot{m}_E = \left(Y_L^a - Y_L^E\right) / \left(Y_L^a - Y_L^D\right) \quad (1)$$

and

$$\dot{m}_p / \dot{m}_E = \left(Y_L^a - Y_L^E\right) / \left(Y_L^a - Y_L^p\right) \quad , \quad (2)$$

respectively, where Y_L stands for the mass fraction of species L, superscripts a, D, p and I denote the ambient air, the opening jet, the small hood and the exhaust duct, respectively. In thi study, O_2 and CO_2 are employed as the tracer gas species L. The mass fractions of species Y_L cannot be directly measured by usual gas analyzers but need to be calculated from the volum fractions of species measured. Letting M_L be the molecular weight of species L, the relationshi

between the mass fraction Y_L and volume fraction X_L of species L at an arbitrary measurement position is given as follows:

$$Y_L = M_L X_L / \left(M_{O_2} X_{O_2} + M_{CO_2} X_{CO_2} + M_{N_2} X_{N_2} + M_{H_2O} X_{H_2O} \right) \tag{3}$$

However, the volume fractions of N_2 cannot be measured and H_2O is filtered out before the gas analyzers in this series experiment. Taking these conditions into account, the formulas for calculating Y_{O_2} and Y_{CO_2} at an arbitrary location from the gas volume fractions measured are developed for the case of methanol fuel (CH_3OH), which is used as the fire source in this series of experiments. Using the stoichiometric relationship between O_2 consumption and generation of H_2O in complete combustion of methanol, we obtain

$$Y_{O_2} = 24\left(4X_O^a - 3\right)X_{O_2}^A / \left\{ \left(21 - 10X_{O_2}^a\right)\left(4X_{O_2}^A - 3\right) + \left(13X_{O_2}^A - 12X_{CO_2}^A\right)\left(4X_{O_2}^a - 3\right) \right\} \tag{4}$$

Instead, the stoichiometric relationship between generations of CO_2 and H_2O may be also invoked to yield

$$Y_{CO_2} = 11\left(1 + 2X_{CO_2}^a\right)X_{CO_2}^A / \left\{ \left(7 + 5X_{CO_2}^a\right)\left(1 + 2X_{CO_2}^A\right) + \left(X_{O_2}^A - X_{CO_2}^A\right)\left(1 + 2X_{CO_2}^a\right) \right\} \tag{5}$$

In Eqns.(4) and (5), X_L^A stand for the volume fraction of species L $(L = O_2, CO_2)$ measured by the gas analyzer. As for the mass fractions of species in ambient air, assuming that the mass fraction of H_2O in fresh air is negligible, we have

$$Y_{O_2}^a = 8X_{O_2}^a / \left(7 + X_{O_2}^a + 4X_{CO_2}^a\right) \tag{6}$$

and

$$Y_{CO_2}^a = 11X_{CO_2}^a / \left(7 + X_{O_2}^a + 4X_{CO_2}^a\right) \tag{7}$$

Hence, using Eqns.(4) and (6), or Eqns.(5) and (7), in Eqns.(1) and (2) , respectively, the mass flow rates of an opening jet and an opening jet plume can be obtained[3].

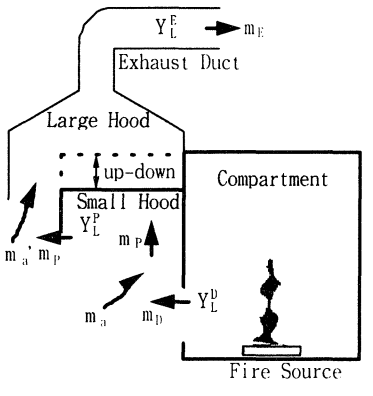

FIGURE 1 Schematic Diagram of The Measurement Method

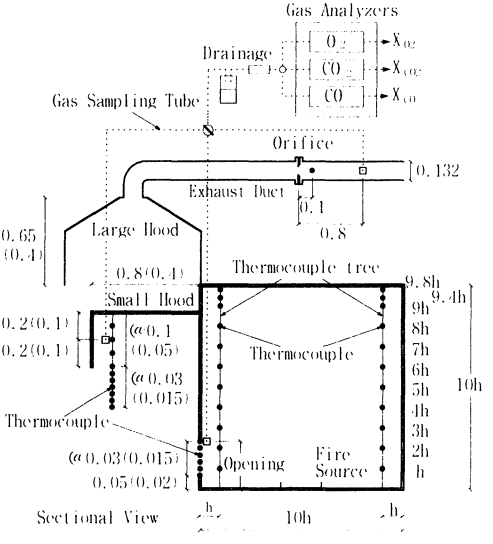

FIGURE 2 Experimental Setup for the Measurement
Numbers indicate dimensions in meter for medium scale (small scale)
10h=1.5m for medium scale (0.5m for small scale)

3. EXPERIMENTS

3.1 Model Fire Compartments

The two geometrically similar experimental setups as shown in Figure 2 are used in this series o experiments. The inside measurements of the small scale and the medium scale cubic fir compartments are 0.5m and 1.5m, respectively. Methanol in pans of different sizes are placed o the floor of the compartment and burned as the fire source. The size and geometry of the openin of the compartment are changed using panels having different openings. The small hood, c changeable elevations, is installed above the opening. The large hood is installed above the smal hood to capture all the gases overflowing from the small hood. At the top of the large hood, duct equipped with a mechanical fan is installed to extract the gases and an orifice is provided i the duct to measure the extraction rate of the gases.

3.2 Measurements

(1) Temperatures

The temperatures are measured in the compartment, in the opening, in the small hood, below th small hood, in the large hood and in the duct. The locations of the thermocouples for th temperature measurements are shown in Figure 2. The temperatures at the opening wer measured by the thermocouples arrayed at 3cm from one of the edges of opening with 3cm an 1.5cm spacing in the medium and the small scale setups, respectively. The temperatures belov the bottom of the small hood were measured by 10 thermocouples arrayed vertically with 3.0 an 1.5cm spacing in the medium scale and the small scale setups, respectively.

(2) Gas concentrations

The concentrations of O_2, CO_2 and CO are measured at the opening in the compartment, in th small hood and in the duct after steady state has been confirmed in these points.

(3) Orifice Pressure

The pressure difference at the orifice is measured to obtain the gas flow rate through the duct.

3.3 Experimental Conditions

The conditions of the opening, fire source and the height of the small hood in the medium an small scale experiments are shown in Tables 1(a) and (b), respectively. The experiments wer conducted for every combination of these conditions. Incidentally, the height of the small hood i the tables means the distance from the top of the opening to the bottom of the small hood.

TABLE 1 Experimental Conditions

(a) Medium Scale Experiment

Opening Shape		Fire Source Condition		Small Hood
Width B(m)	Height H(m)	Diameter (m)	Heat Release Rate (kW)	Height (m)
0.15	0.30	0.1	4.0	0
0.15	0.45			0.05
0.30	0.15	0.2	6.6	0.1
0.30	0.30			0.2
0.30	0.45	0.2	10.6	0.3
0.45	0.15			0.4
0.45	0.30			0.5
0.45	0.45			

(b) Small Scale Experiment

Opening Shape		Fire Source Condition		Small Hood
Width B(m)	Height H(m)	Diameter (m)	Heat Release Rate (kW)	Height (m)
0.10	0.15	0.0		0
0.10	0.20			0.05
0.15	0.15	0.1	1.2	0.10
0.15	0.20			0.15
0.20	0.15			0.20
0.20	0.20			0.25

3.4 Experimental Procedure

The data acquisition was started after a steady state condition has been confirmed by monitoring each measurement on a personal computer screen. While the temperatures and the pressure were continuously measured, the gas concentrations were measured by a set of gas analyzers by sequentially switching the gas probe to the compartment, the small hood and the duct, in order to avoid errors caused by small differences between gas analyzers. Incidentally, the changes of the temperatures and the gas concentrations during this period were very trivial. This procedure was repeated every time the condition of experiments is changed.

3.5 Results of Experiments

Figures 3.(a) and 3.(b) show some examples of the mass flow rates of opening jet $\dot{m}_{in}$ and opening jet plumes $\dot{m}_p$ obtained from the measurements in the medium and the small scale experiments, respectively. Needless to mention, the mass flow rates of the opening jet plumes $\dot{m}_p$ increase with the height of the small hood while the flow rates of the opening jets $\dot{m}_{in}$ remain constant regardless the height. The flow rates of the opening jet plumes $\dot{m}_p$ also increase as the size of the fire source becomes large. This is because larger fire sources cause higher opening jet temperature and hence stronger buoyancy of opening jet plumes.

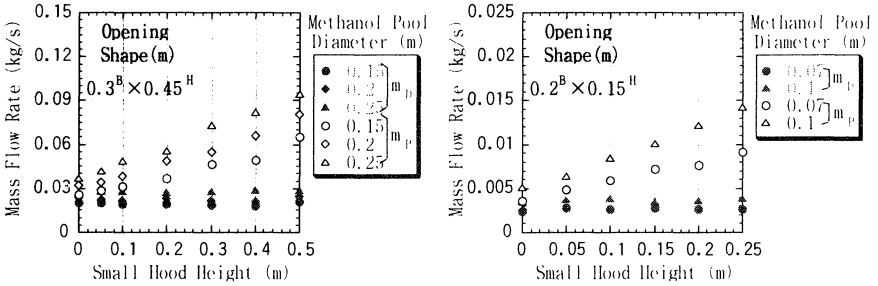

(a) Medium Scale Experiment (b) Small Scale Experiment

FIGURE 3 Flow Rates of Opening Jets and Opening Plumes v.s. the Small Hood Height

4. ANALYSES OF THE EXPERIMENTAL RESULTS

4.1 Existing opening jet plume

As is well known, the mass flow rate of fire plume $\dot{m}_p$ can be calculated as

$$\dot{m}_p = C\dot{Q}^{1/3}(Z + Z_0)^{5/3} \tag{8}$$

where $\dot{Q}$ is the heat release rate of fire source, and Z and Z_0 are the height from the fire source and the distance of the virtual point heat source, respectively. C is the constant which takes a value about $C \approx 0.07 \sim 0.08$[4].

In BRI2 etc., a two layer zone fire model, the flow rates of opening jet plumes are estimated by simply applying this formula with some modification: The effective height of the source of the plume Z_0, which is where the plume mass flow rate of the vertically modeled plume becomes

the same as the opening jet mass flow rate, is regarded to be located at the mean height of th opening jet, i.e. $(H - Z_n)/2$ below the top of the opening, where H is the height of the openin and Z_n is the height of the neutral plane at the opening; The heat release rate $\dot{Q}$ in Eqn.(8) i substituted by the heat flow rate of the opening jet at elevated temperature $\dot{Q}_D$ calculated by

$$\dot{Q}_D = c_p \dot{m}_D (T_D - T_\infty) \tag{9}$$

where c_p is specific heat of gas at constant pressure, $\dot{m}_D$ is the mass flow rate of the opening je and T_D and T_∞ are the opening jet temperature and ambient temperature, respectively; Th distance of the virtual point heat source Z_0 is calculated by letting $Z = 0$ in Eqn.(8) as[5, 6]

$$Z_0 = \left(\frac{\dot{m}_D}{C \dot{Q}_D^{1/3}} \right)^{3/5} = C' \left(\frac{\dot{m}_D}{\dot{Q}_D^{1/3}} \right)^{3/5} \tag{10}$$

where $C' = C^{-3/5} \approx (4.6 - 4.9)$.

4.2 Dependence of plume mass flow rate on heat addition rate

If the existing opening jet plume entrainment model in BRI2 as described in the above is valid, i follows from Eqns. (8) ~ (10) that

$$\dot{m}_p^{3/5} - \dot{m}_D^{3/5} = C^{3/5} \dot{Q}_D^{1/5} Z \tag{11}$$

that is $\dot{m}_p^{3/5} - \dot{m}_D^{3/5}$ is in proportion to $\dot{Q}_D^{1/5}$ for any given entrainment height. Figure 4 plot $\dot{m}_p^{3/5} - \dot{m}_D^{3/5}$ versus $\dot{Q}_D$ measured in some of the medium and small scale experiments. Here, $\dot{Q}_D$ is calculated by Eqn.(9) where T_D was taken as the average of the temperature recordings of th thermocouples located between the upper end of the opening and the neutral plane, which wa determined from the temperature profile of an opening jet using N% method(N=10 in this paper [7]. It can be seen in Figure 4 that $\dot{m}_p^{3/5} - \dot{m}_D^{3/5}$ is almost proportional to $\dot{Q}_D^{1/5}$ in any height of th small hood.

4.3 Effective height of the source of the opening jet plume

From the above findings, it is presumed that the opening jet plumes show similar behavior wit fire plumes so that they can be modeled into vertical plumes as illustrated in Figure 5 as long as

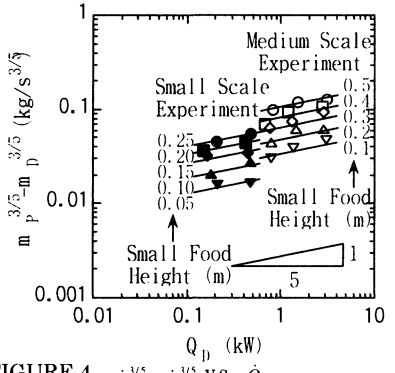

FIGURE 4 $\dot{m}_p^{3/5} - \dot{m}_D^{3/5}$ v.s. $\dot{Q}_D$ at each Height of Small Hood

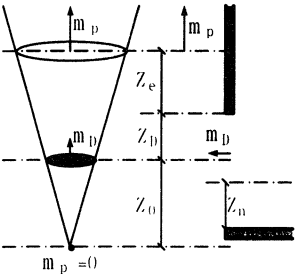

FIGURE 5 Modeling of Opening a Jet Plume into a Vertical Plume

the plume flow rates are concerned. Here, we define the effective height of the source of the plume Z_D as the distance from the top of the opening to the height where the plume mass flow rate of the vertical plume model is the same as the opening jet mass flow rate. In Figure 6 the ratios of the plume flow rates to the opening jet flow rates $\dot{m}_p / \dot{m}_D$ in the medium and small scale experiments with different conditions are plotted versus $Z_c/(H-Z_n)$, where Z_c is the distance from the top of the opening to the bottom of the hot gas layer in the small hood, which is determined by applying N% method(N=10 is used in this study)[7] to the temperature profiles below the small hood. The sharp temperature profiles below the small hood as exemplified in Figure 7 imply that the bottom of the hot gas layer can be determined fairly accurately. As can be seen in Figure 6, the increase of $\dot{m}_p / \dot{m}_D$ with $Z_c/(H-Z_n)$ vary depending on the opening conditions but the values of $\dot{m}_p / \dot{m}_D$ for all the cases are found to converge to 1 at the same height, that is where $Z_c|_{\dot{m}_p/\dot{m}_D=1}/(H-Z_n) = -2/3$. Hence the effective height of the plume source Z_D is commonly given as

$$Z_D \left(\equiv -Z_c|_{\dot{m}_p/\dot{m}_D=1} \right) = \frac{2}{3}(H-Z_n) \tag{12}$$

regardless the opening conditions. Hence, the location of the effective source of the opening jet plume source found in this study is somewhat lower than that in BRI2.

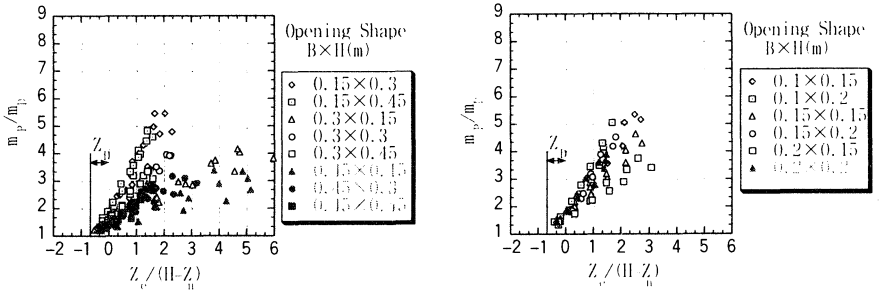

(a) Medium Scale Experiment (b) Small Scale Experiment

FIGURE 6 Effective Height of The Source of Opening Jet Plume

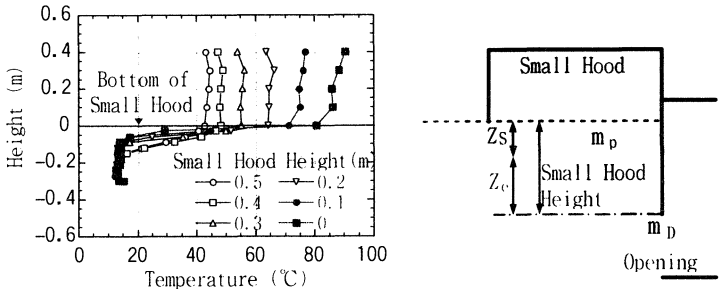

FIGURE 7 Temperature Profile Below The Small Hood

4.4 Virtual point heat source

Based on the above discussion, it is possible to assume that the formula for the mass flow rate c opening jet plume take the form as follows:

$$\dot{m}_p = kQ_D^{1/3}(Z_c + Z_D + Z_0)^{5/3} \tag{13}$$

The coefficient k and the distance of virtual point heat source Z_0 are unknown in this formul However, transforming Eqn.(13) as

$$\left(\dot{m}_p / \dot{Q}_D^{1/3}\right)^{3/5} = k^{3/5}(Z_c + Z_D) + k^{3/5}Z_0 \tag{14}$$

and noting that that $k^{3/5}$ and $k^{3/5}Z_0$ are given as the slope and the interception on the coordinate respectively, in the plots of $\left(\dot{m}_p / \dot{Q}_D^{1/3}\right)^{3/5}$ versus $Z_c + Z_D$ as illustrated in Figure 8, the height o the virtual point heat source can be calculated. Figure 9 plots the distance of the virtual point hea source Z_0 thus obtained versus $\dot{m}_D / \dot{Q}_D^{1/3}$. The regression line of the data in this figure may b expressed in terms of the formula as follows:

$$Z_0 = 5.0\left(\dot{m}_D / \dot{Q}_D^{1/3}\right)^{3/5} \tag{15}$$

that is the Z_0 found in this study is slightly larger than the Z_0 employed in BRI2 etc.[5, 6] which is given by Eqn.(10).

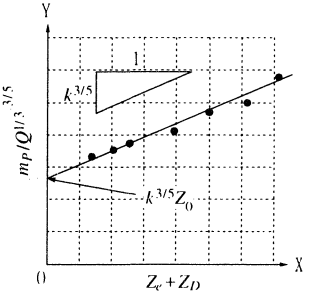

FIGURE 8 Schematic for Obtaining Virtual Point Source

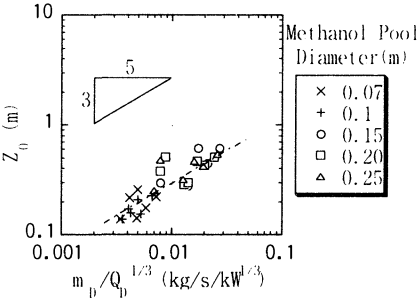

FIGURE 9 Relationship between $\dot{m}_p / \dot{Q}_D^{1/3}$ and Virtual Point Source

5. SCALING OF OPENING JET PLUME FLOW RATE

5.1 Non-dimensional Formula for Opening jet Plume Flow Rate

In the above, the flow rates of opening jet plume were investigated based on the results of the medium and the small scale experiments. However, a scaling parameter need be established in order to apply the results to the opening jet plumes with realistic scales. Letting D be the characteristic length, Eqn.(13) can be transformed into a non-dimensional formula as follows:

$$\mu_p = \kappa\left(\frac{Z_c + Z_D + Z_0}{D}\right)^{5/3} \tag{16}$$

where κ is a coefficient and μ_p is the non-dimensional plume mass flow rate defined as

$$\mu_p \equiv \frac{\dot{m}_p / \rho_\infty \sqrt{g} D^{5/2}}{\dot{Q}_D^{*1/3}} \tag{17}$$

with the non-dimensional opening jet heat flow defined for the characteristic length D as

$$\dot{Q}_D^* \equiv \dot{Q}_D / \left(c_p \rho_\infty T_\infty \sqrt{g} D^{5/2} \right) \tag{18}$$

where ρ_∞ and g are ambient air density and acceleration due to gravity, respectively.

Using that $\dot{m}_p = \dot{m}_D$, hence $\mu_p = \mu_D$, at $Z_c + Z_D = 0$ in Eqn.(16) yield the relationship as follows:

$$\mu_D = \kappa (Z_0 / D)^{5/3} \tag{19}$$

where μ_D is the non-dimensional mass flow rate of the opening jet

$$\mu_D \equiv \left(\dot{m}_D / \rho_\infty \sqrt{g} D^{5/2} \right) / \dot{Q}_D^{*1/3} \tag{20}$$

5.2 Non-dimensional Virtual Point Heat Source

The unknown parameters in the above equations i.e. κ and Z_0 / D can be obtained by transforming Eqn.(16) as

$$\mu_p^{3/5} = \kappa^{3/5} \left(\frac{Z_c + Z_D}{D} \right) + \kappa^{3/5} \left(\frac{Z_0}{D} \right) \tag{21}$$

in the same manner as Eqn.(14) and applying a procedure similar to that illustrated by Figure 8. However, the characteristic length D has to be specified in order to actually calculate the κ and Z_0 / D. Two lengths were tried as the characteristic length D in this study. One is the opening width B and the other is the effective opening jet radius r_0 defined as

$$r_0 \equiv \sqrt{B(H - Z_n)/\pi} \quad , \tag{22}$$

which is similar to Yokoi's effective opening jet diameter[8]. Using the results obtained by this procedure, the non-dimensional distance of virtual point heat source can be determined. For both of the characteristic lengths r_0 and B, the coefficient κ was found to take the same value of 0.19. So, it follows from Eqn.(19) that

$$Z_0 / r_0 = Z_0 / B = \left(\mu_D / 0.19 \right)^{3/5} \tag{23}$$

Figures 10(a) and (b) show the relationship between μ_D and the non-dimensional distances of virtual point heat source defined for r_0 and B, respectively. Curiously, the non-dimensional virtual point source distance Z_0 / r_0 for the characteristic length r_0 does not vary much with μ_D and seems to take an average value of about 3, i.e. $Z_0 / r_0 \approx 3$. In terms of the opening jet area

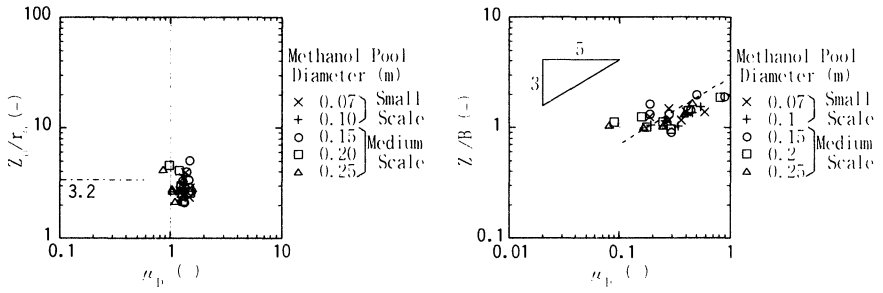

(a)Effective Doorjet Radius as the Characteristid Length

(b) Opening Width as the Characteristid Length

FIGURE 10 Non-dimensional Virtual Point Source Distance and Opening Flow Rate

$A_D (= \pi r_0^2)$, this relationship may be expressed as $Z_{v0} \approx 1.7\sqrt{A_D}$, in other words, close to Thomas' virtual point heat source vertical plumes. On the other hand, the relationship of Z_{v0}/B and μ_D in Figure 10(b) seems to be expressed by Eqn.(23) reasonably well.

5.3 Scaling of Flow Rates of Opening Jet Plumes

Figure 11 plots $\dot{m}_p / Q_D^{1/3}$ versus $Z_v + Z_D + Z_0$ based on the results of the medium and the small scale experiments with different heat release rates and opening geometry. According to Figure 11 the values of $\dot{m}_p / Q_D^{1/3}$ scatter depending on the experimental conditions and tend to increase as the shape of the opening becomes vertically more slender. Figure 12 plots the non-dimensional plume mass flow rates defined for the characteristic length of r_0 versus the non-dimensional height $(Z_v + Z_D + Z_0)/r_0$. As can be seen in Figure 12, the extent of the scattering of the data decreases compared with Figure 11, but the scattering may not be satisfactory. Figure 13 plots the non-dimensional plume mass flow rates defined for the characteristic length of B versus the non-dimensional height $(Z_v + Z_D + Z_0)/B$. It can be seen that the scattering of the data has remarkably decreased and all the data nearly collapse onto a single line in each of the medium and the small scale experiments.

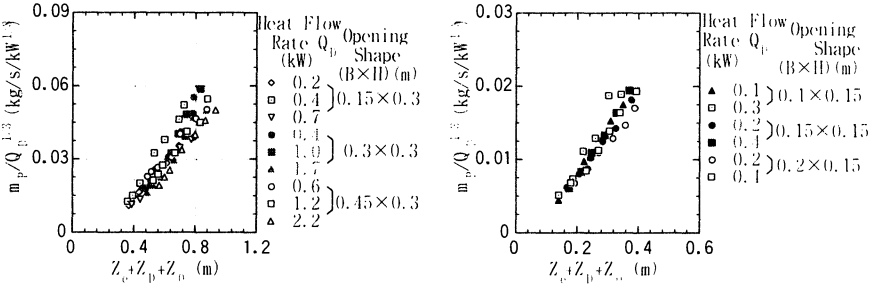

(a) Medium Scale Experiment (b) Small Scale Experiment

FIGURE 11 Mass Flow Rate of Opening Jet Plume v.s. Entrainment Height

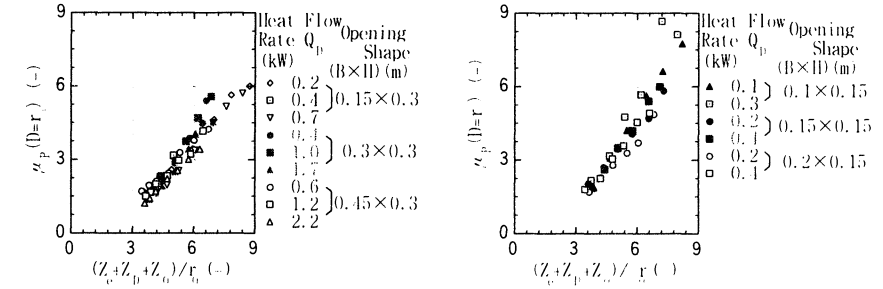

(a) Medium Scale Experiment (b) Small Scale Experiment

FIGURE 12 Non-dimensional Mass Flow Rate of Opening Jet Plume v.s. Non-Dimensional Entrainment Height($D=r_0$)

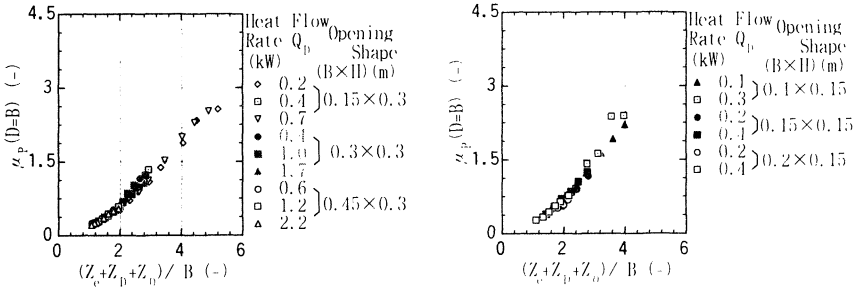

(a) Medium Scale Experiment (b) Small Scale Experiment

FIGURE 13 Non-dimensional Mass Flow Rate of Opening Jet Plume v.s. Non-Dimensional Entrainment Height(D=B)

It is implied from the results of Figures 11~13 that the non-dimensional mass flow rate defined using the characteristic length B is the best scaling parameter of the three. So all the data from the medium and the small scale experiments are plotted together in Figure 14, where n indicates the aspect ratio of the opening jet, defined as $n \equiv (H - Z_n)/B$. It can be said that the non-dimensional mass flow rates exhibit an excellent correlation with the non-dimensional height, regardless the conditions of the opening geometry and the fire source.

6. CONCLUSION

The mass flow rates of opening jet plumes in this series of experiments are best correlated as the relationship between the non-dimensional mass flow rate and the non-dimensional height when defined using the width of opening B as the characteristic length. The relationship shown in Figure 14 may be expressed as

$$\mu_p = 0.19\left(\frac{Z_e + Z_D + Z_0}{B}\right)^{5/3} \tag{24}$$

Here, Z_e is the height from the top of an opening and μ_p is the non-dimensional plume mass flow rate defined as

$$\mu_p \equiv \frac{\dot{m}_p / \rho_\infty \sqrt{g} B^{5/2}}{\dot{Q}_D^{*1/3}} \tag{25}$$

and the non-dimensional effective height of the plume source and non-dimensional height of the virtual point source are given as

$$\frac{Z_D}{B} = \frac{2}{3}\left(\frac{H - Z_n}{B}\right) \tag{26}$$

and

$$Z_0 / B = (\mu_D / 0.19)^{3/5} \quad , \tag{27}$$

respectively. Furthermore, the non-dimensional mass flow rate and heat flow rate of the opening jet are given by

$$\mu_D \equiv \left(\dot{m}_D / \rho_\infty \sqrt{g} B^{5/2}\right) / \dot{Q}_D^{*1/3} \tag{28}$$

and

$$\dot{Q}_D^* \equiv \dot{Q}_D / \left(c_p \rho_\infty T_\infty \sqrt{g} B^{5/2} \right) \tag{29}$$

respectively.

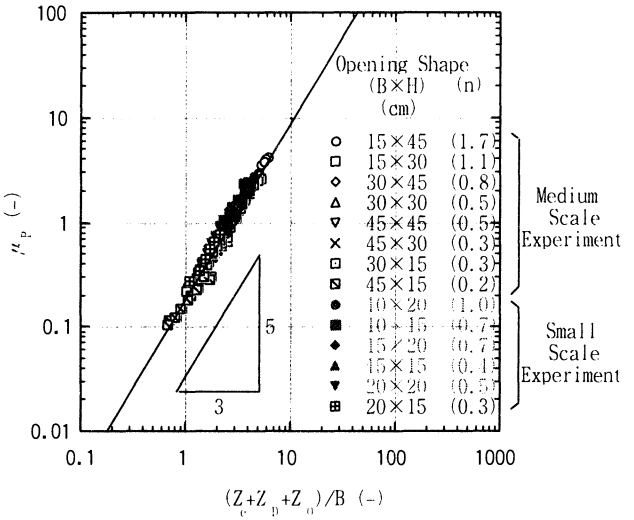

FIGURE 14 Non-dimensional Mass Flow Rate of Opening Jet Plume v.s. Non-Dimensional Entrainment Height(D=B)

REFERENCE

[1] Friedman, R.: "An International Survey of Computer Models for Fire and Smoke", Journal o Fire Protection Engineering, 4 (3), pp. 81-92, 1992.

[2]Cetegen, B.M., Zukoski, E. E. and Kubota, T. : "Entrainment in the Near and Far Field of Fir Plumes", Combustion Science and Technology, Vol. 39, pp. 305-331, 1984.

[3] Yamaguchi, J., Yamada, S., Tanaka, T. and Wakamatsu, T.: "Measurement for Mass Flow Rate of Door Jet in Compartment Fire", Transaction of AIJ, No. 501, pp.1-7, 1997. (in Japanese)

[4] Zukoski, E. E., Kubota, T and Cetegen, B.M: "Entrainment of Fire Plumes", Fire Safet Journal, 3(1980/1981), pp. 107-121, 1981

[5] Tanaka, T.: "A Model of Multiroom Fire Spread", Fire Science and Technology, Vol.3, No.2 pp. 105-121, 1983.

[6] Nakamura, K. and Tanaka, T.: "Predicting Capability of a Multiroom Fire Model", Fire Safet Science, Proc. of the 2nd Int'l Symposium, pp. 907-916, 1989.

[5] Yamaguchi, J., Hosozawa, T., Tanaka, T. and Wakamatsu, T.: "Investigation into Entrainmen of Opening Jet Plume", Transaction of AIJ, No. 511, pp.1-8, 1998. (in Japanese)

[7] Cooper, L. Y., Harkeroad, Quintiere, J.G. and Rinkenen, W.: "An Experimental Study o Upper Hot Layer Stratification in Full-Scale Multiroom Fire Scenarios", Journal of Heat Transfer Vol.104, pp. 741-749, 1982.

[8] Yokoi, S. : "Study on the Prevention of Fire-Spread Caused by Hot Upward Current", Repor of The Building Research Institute, BRI, 1960.